COBEM 2023 27TH INTERNATIONAL CONGRESS OF MECHANICAL ENGINEERING

ABCM Brazilian Society of Mechanical Sciences and Engineering
27th ABCM International Congress of Mechanical Engineering
December 04-08, 2023, Florianópolis-SC, Brazil

COB-2023-0634
AERODYNAMIC OPTIMIZATION OF WING-MOUNTED ROTOR CONFIGURATION FOR eVTOLS

Gilberto Bueno Luque Filho
Instituto Tecnológico de Aeronáutica, DCTA/ITA, São José dos Campos, SP, Brazil
gbueno.luque@gmail.com

João Luiz F. Azevedo
Instituto de Aeronáutica e Espaço, DCTA/IAE/ALA, São José dos Campos, SP, Brazil
joaoluiz.azevedo@gmail.com

Abstract. *This paper aims to address the complexity of rotor-airframe interaction in the context of gradient-based optimization applied to non-conventional configurations of electric Vertical Take-Off and Landing vehicles. The main objective is to enhance understanding of the influence of rotor-airframe interaction on aerodynamic design and how these effects can lead to significantly different configurations. To achieve this, a low-fidelity tool based on the Vortex-Lattice Method with nonlinear viscous corrections has been developed. The tool incorporates a three-dimensional Free Form Deformation method for geometry parameterization, directly implemented in Python. Aerodynamic calculations are performed using a Fortran code, which is integrated into the Python optimization process using a Python script and the Scipy Python library. The established framework includes a nonlinear aerodynamic code, FFD-based parameterization, and an optimization framework that captures stall trends and the influence of unsteady wakes during the optimization process. Results obtained are encouraging, highlighting the potential of this research. Addressing the challenges of rotor-airframe interaction during the conceptual design phase and optimizing non-conventional aircraft is a crucial topic in the aeronautic industry. This paper contributes to the understanding of this coupling, aiding informed design decisions.*

Keywords: *eVTOL, Rotor-Wing interaction, Vortex Lattice Method, Free-Form-Deformation, Gradient-based optimization*

1. INTRODUCTION

In recent years, there has been a significant increase in research regarding Electric Vertical Takeoff and Landing (eVTOL) vehicles. This advancement is spurred, in part, by the long-term objectives of the aviation industry, which aspires to achieve a substantial reduction in net carbon dioxide emissions by 2050, compared to the levels recorded in 2005. Moreover, this development aligns harmoniously with the extensive financial forecasts projecting the total market value of electric Vertical Take-Off and Landing (eVTOL) technology to reach a remarkable sum of $9 trillion by the year 2050 (Erhard and Alonso, 2022).

Those vehicles, which usually have multiple rotors that are often located on wings, present several challenges for aerodynamic engineers, particularly regarding the interaction between rotors and wings. To address these challenges, researchers have been using advanced computational tools such as Computational Fluid Dynamics (CFD) simulations and wind tunnel experiments to gain a better understanding of the complex aerodynamic interactions. These expensive yet high-fidelity approaches directly solve entire flow fields, including wing, rotor blades and downstream regions, to predict unsteady and transient phenomena. With the significant growth in computing performance and resources, researchers in both industry and academia have been striving to simulate various rotorcraft configurations using different CFD methods.

Despite numerous modifications aimed at improving the efficiency of CFD methods, they remain impractical for industrial designers seeking rapid feedback to optimize their models due to their high computational costs and complex equation setup, mainly in the preliminary design phase of the product. Consequently, in the realm of comprehensive wing-mounted configuration analysis codes, vortex methods have been widely embraced due to their inherent capabilities. These methods encompass a range of approaches for modeling the lifting surface, including the lifting line theory (LLT), Weissinger's LLT (extended lifting-line theory), the lifting surface method, and the source-doublet panel method. LLT and Weissinger's LLT utilize a simplistic representation of the wing model, employing vortex singularities known as horseshoe vortex filaments along the spanwise direction. Nonetheless, these models exhibit limitations in capturing the intricate three-dimensional effects on the rotor blade and wings, as they solely represent the lifting surface using a solitary chordwise vortex element.

In contrast, the lifting surface method, also known as the vortex lattice method (VLM), addresses the lifting surface curvature by incorporating both chordwise and spanwise distributions of vortex ring elements on the actual cambered surface. Consequently, VLM significantly improves the representation of the flow three-dimensionality, despite the in-

viscid and irrotational fluid assumption. The aforementioned challenges, for both methodologies, can be mitigated by incorporating the two-dimensional information pertaining to the sections of the lifting surface through methodologies like decambering (Mukherjee and Gopalarathnam, 2006).

In this paper, the complexity of the rotor-airframe interaction will be addressed from the perspective of gradient-based optimization of non-conventional configurations of eVTOL vehicles through the use of a low-fidelity tool. The main objective of this work is to develop the understanding of the influence of the rotor-airframe interaction over the aerodynamic design, and how the consideration of these effects can lead to considerably different configurations. Therefore, a low-fidelity tool developed by the authors, based on the Vortex-Lattice Method (VLM) with nonlinear viscous corrections, is used. For the geometry parameterization, a three-dimensional Free Form Deformation (FFD) method is implemented directly in Python. The aerodynamic calculation is performed by a Fortran code, which is, then, imported to the Python optimization process through a Python script and optimized using the Scipy Python library. The nonlinear aerodynamic code, the parameterization through the FFD method and the optimization framework are already implemented, enabling aerodynamic results that capture stall trends and the influence of unsteady wakes in the optimization process. Results obtained are encouraging, highlighting the potential of this research. The conceptual design phase and the optimization of non-conventional aircrafts with rotor-airframe interaction is a challenging topic for the aeronautic industry. The paper aims to address the understanding of this coupling for the design phase.

2. THEORETICAL FORMULATION

2.1 Unsteady Vortex Lattice Method

The Vortex Lattice Method (VLM) represents a computational approach within the realm of fluid dynamics. It assumes an inviscid, irrotational, and incompressible flow surrounding the body, neglecting the influence of viscosity, flow separation at the leading edge, and compressibility at high Mach numbers. Under these aforementioned assumptions, a velocity potential, denoted by Φ, can be established. In this context, the continuity equation in the inertial frame can be mathematically expressed as Laplace's equation, Eq. (1).

$$\nabla^2 \Phi = 0 \, . \tag{1}$$

The solutions to Laplace's equation encompass the source and doublet elements, serving as the fundamental solutions, which have the strengths σ and μ, respectively. By integrating the contributions from these fundamental solutions distributed across the body's surface, a general solution can be obtained as follows:

$$\Phi = \frac{1}{4\pi} \int_{body+wake} \mu \hat{\mathbf{n}} \cdot \nabla \left(\frac{\mathbf{1}}{\mathbf{r}} \right) ds - \frac{1}{4\pi} \int_{body} \sigma \left(\frac{1}{r} \right) ds. \tag{2}$$

To approximate lifting surfaces as thin structures, the source term is disregarded, and a constant-strength doublet panel is employed, serving as an analogous closed vortex lattice with an equivalent circulation strength Γ . The correspondence between the utilization of doublets and vortex rings has been demonstrated by Hess and Smith. (1967). The discretization of lifting surfaces involves a lattice of short, straight vortex segments, which form enclosed triangular or quadrilateral vortex loops. These panels correspond to the bound vortex sheets, (Konstadinopoulos *et al.*, 1985), where vorticity is confined, as depicted in Fig. 1.

The determination of vortex ring element strength relies on the imposition of certain boundary conditions that the flow must adhere to:

1. The magnitude of the local velocity vector, defined in an inertial frame fixed to the fluid, diminishes towards zero in regions distant from the body, $|\vec{V} \rightarrow 0|$, a condition automatically fulfilled by computing velocities using the Biot-Savart law.

2. A no-penetration condition is enforced at the control points, situated at the geometric centroids of the lifting panels.

3. According to the Kelvin-Helmholtz theorem for inviscid fluids, the angular momentum cannot change, and thus the circulation Γ around a fluid curve enclosing the wing and its wake is conserved and does not vary in time (Katz and Plotkin, 2004). Hence, over the wake, $\frac{D\Gamma}{Dt} = 0$. Consequently, the total circulation variation along any closed loop along the wake must be nullified. This condition facilitates the convective motion of a force-free wake.

4. The Kutta condition states that flow leaves tangentially, with a finite velocity, the trialling edge. In the UVLM, the unsteady Kutta condition is realized by shedding vorticity generated along a sharp trailing edge into the wake (Konstadinopoulos *et al.*, 1985). By enforcing the elimination of pressure jumps across the trailing edge, the fluid can depart smoothly from the surface. The nodes within the wake are free to move at the local fluid particle speed,

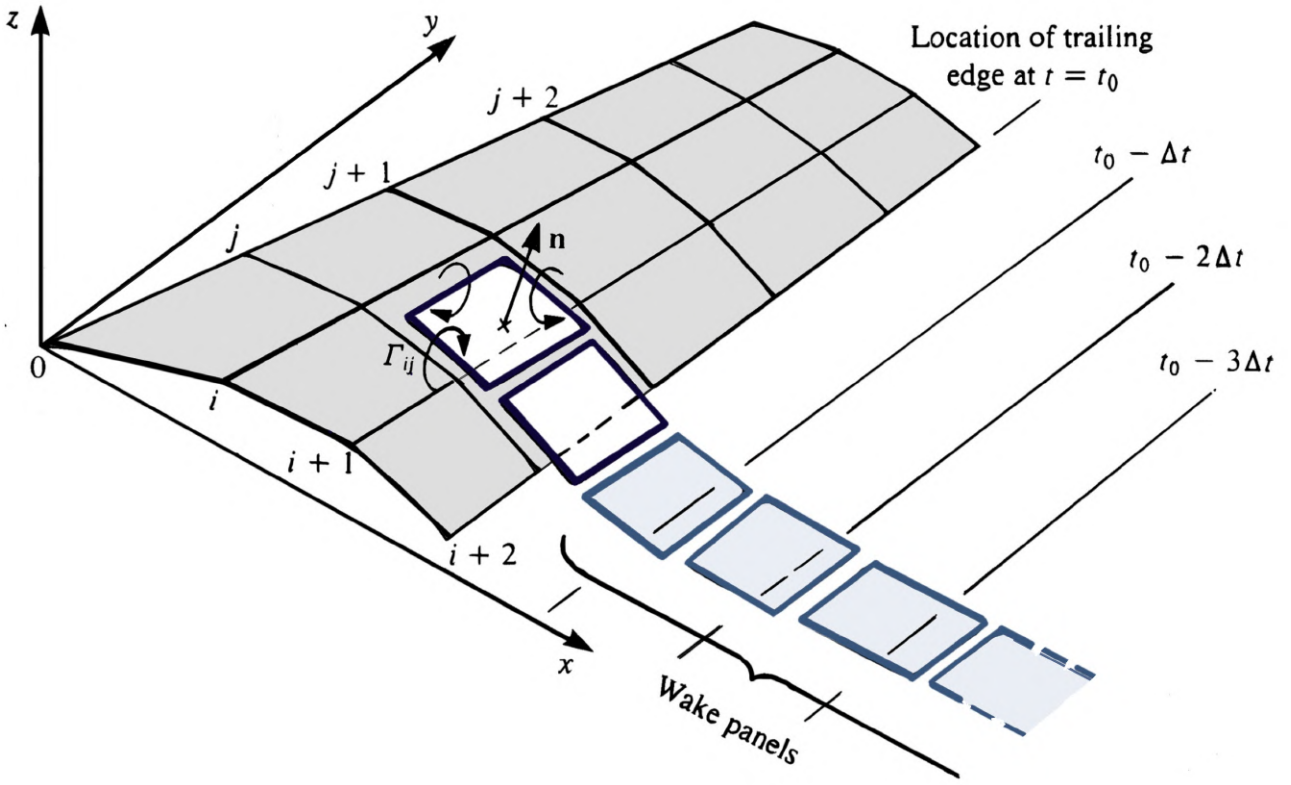

Figure 1. Surface representation in the UVLM with a discretized thin lifting surface and vortex ring element.

maintaining a force-free wake. While some researchers employ predictor-corrector approaches (Bhagwat and Leishman, 2000) and/or high-order schemes (Wie *et al.*, 2009) to calculate wake positions at each time step, the current work utilizes the explicit Euler method to convect fluid particles within the wake.

The time-dependent kinematic velocity, denoted by the term $\vec{V}$, is a composed of the system's velocity V_∞, the relative velocity of the body, and the rotational velocity of the body's frame $\vec{\Omega}\times\vec{r}$, where $\vec{r}$ is the distance between the control point and rotation center of the aircraft and $\vec{\Omega}$ is the maneuver velocity. Furthermore, there are additional velocity components, $V_{ind,bound}$ and $V_{ind,wake}$, which are the induced velocities caused by the lifting surfaces and wake vortices, respectively.

The application of the no-penetration boundary condition to the vortex sheet simplifies the task of determining the strengths of the vortices to a system of linear algebraic equations. Therefore, the equation for the calculation of the circulation of the bound vortices can be written as

$$\begin{bmatrix} a_{1,1} & a_{1,2} & \cdots & a_{1,n} \\ a_{2,1} & a_{2,2} & \cdots & a_{2,n} \\ \vdots & \vdots & \ddots & \vdots \\ a_{n,1} & a_{n,2} & \cdots & a_{m,m} \end{bmatrix} \begin{Bmatrix} \Gamma_1 \\ \Gamma_2 \\ \vdots \\ \Gamma_m \end{Bmatrix} = \begin{Bmatrix} RHS_1 \\ RHS_2 \\ \vdots \\ RHS_m \end{Bmatrix}, \tag{3}$$

where

$$RHS_i = -\left(\vec{V}_\infty + \vec{V}_{ind,wake} - \vec{\Omega}\times\vec{r}\right)_i \cdot \mathbf{n}_i\,, \tag{4}$$

and

$$a_{i,j} = \left(\vec{V}_{ind,bound}\right)_{ij} \cdot \mathbf{n}_i \tag{5}$$

In the previous equation, $\mathbf{n}_i$ is the outward unit normal vector of the $i-th$ panel surface. The circulation of the bound vortices, Γ_i and, consequently, the self-induced velocity by the rotor blade and wing, can be expressed as a combination of influence coefficients $a_{i,j}$. These influence coefficients are defined as the velocity components normal to the surface induced by the $j-th$ vortex ring element with unit strength at the collocation point of the $i-th$ vortex ring element. On the right-hand side of the equation, the contributions of wake-induced velocity and body kinematic velocities are incorporated. For a comprehensive understanding of the derivation of the Vortex Lattice Method, refer to Katz and Plotkin (2004), which provides a detailed explanation.

2.2 Nonlinear Viscous Correction

In the realm of linear aerodynamic prediction methods, the expansion to encompass nonlinear and poststall lift curves can be categorized into two main types: the iterative Γ-distribution approach and the α-adjustment approach. In the iterative Γ-distribution approach, an initial assumption is made regarding the lift distribution on the wing, which is subsequently refined through iterative corrections by determining the effective angle of attack, α, distribution based on the characteristics of the nonlinear airfoil lift curve. On the other hand, the α-adjustment approach utilizes the disparity between the nonlinear lift curve of the airfoil and the linear lift curve of potential flow to introduce localized corrections to the α values at each section of the wing. The preferred approach for this research is the iterative technique, which employs a multidimensional Newton iteration scheme to accurately estimate the decambering phenomenon while considering interdependencies between sections. Moreover, it allows for a more comprehensive understanding of the effects of the boundary layer and facilitates accurate predictions in wind tunnel experiments where detailed camber reduction information may not be available.

In this method, the effective decambering of an airfoil is approximated using a function of two variables δ_1 and δ_2.

These two linear functions are added to obtain the final decambering function. The reason for using two variables is that the decambering is determined from two pieces of information: the C_l and the C_m for the α under consideration. To account for these effects, a 2N-dimensional Newton iteration is used to predict the δ_1 and δ_2 at each of the N sections of all of the wings so that, as the iteration advances, the ΔC_l and ΔC_m at these sections approach zero.

While the methodology involves a two-variable decambering function, certain scenarios arise where either the experimental or computational viscous data for the airfoil section lacks information on C_m, or when the decambering approach is applied to an analysis method incapable of computing section pitching moments, e.g., LLT or Weissinger's method (Weissinger, 1947). Consequently, decambering is represented as a function of a singular variable, denoted as δ_1, with δ_2 being assigned a value of zero. Under these circumstances, the viscous decambering function assumes a similarity to that employed in the α-reduction approach. The intricate procedure for the iterative decambering approach, implemented within the scope of this study, is thoroughly detailed by Mukherjee and Gopalarathnam (2006).

In the current study, given the prevalent subsonic flight regime commonly observed in eVTOLs vehicles operation, the influence of compressibility can be reasonably disregarded, thereby enabling a focus solely on the characterization of viscous nonlinear phenomena. Consequently, to establish a comprehensive database pertaining to the aerodynamic properties of two-dimensional sections, the utilization of XFOIL (Drela, 1989), a specialized two-dimensional potential code enhanced with integral boundary layer correction, has been employed as a strategic measure to reduce the computational cost of simulations.

2.3 Mesh Parameterization

In the field of aerodynamic optimization, the significance of geometry or grid parameterization cannot be overstated, as it establishes the fundamental framework for defining the shape and structure of the aerodynamic design. An accurate parameterization scheme enables efficient exploration of the design space and manipulation of design variables to achieve optimal aerodynamic performance. Moreover, a well-defined parameterization methodology ensures the preservation of essential geometric features and constraints, maintaining the desired structural integrity and performance characteristics of the system. Additionally, it facilitates the integration of manufacturing constraints, enhancing the feasibility of the optimized design. In this context of optimization, the design variable of choice is often the geometry itself, represented by numerous grid points in computational fluid dynamics (CFD) simulations. To facilitate gradient-based optimization methods and avoid unsmooth geometry profiles caused by high-frequency modes present in point-wise gradients, it is advantageous to define a new set of design variables based on continuous functions. This approach reduces the number of control points required for geometry optimization while enabling smooth manipulation of the geometry.

In this study, the authors employed the Free Form Deformation (FFD) method for geometry parametrization and deformation, following the original version proposed by Sedeberg and Parry (1986). While commonly used techniques directly manipulate the geometrical object itself, FFD deforms a lattice constructed around the object, thereby manipulating the entire space in which the object is embedded. This approach has primarily been developed in computer graphics but has more recently been employed in aerodynamic shape design problems. The lattice topology takes the form of a cube for three-dimensional objects or a rectangle for two-dimensional objects. One notable advantage of FFD is the flex-

ibility it provides to users in choosing the design parameters, which has been demonstrated to yield good accuracy even with a small number. FFD operates on the entire space that encompasses the deformed objects by defining a reference domain and displacing appropriate control points. This enables users to manipulate the control points of trivariate Bezier volumes, which extend parametric B-spline curves and surfaces into three-dimensional parametric space (Cohen *et al.*, 2002). However, a primary limitation associated with the Free Form Deformation method pertains to the necessity of use of a parallelepiped lattice comprised of control points, as indicated by previous studies of Samareh (2000) and Perry and Balling (1998).

Essentially, this technique initiates by establishing a control lattice that includes the specific region of the geometry intended for morphing. Subsequently, the geometry undergoes a continuous and seamless deformation process by solely displacing the control points within the lattice. The sequential operation, in a three-dimensional scenario, can be divided into three distinct stages. Firstly, after defining a reference domain Ω_0 and a subset that is desired to pertub, $D_0 \subset \Omega_0$, an invertible and differentiable map Ψ is introduced, where the original reference coordinates (x_1, x_2, x_3) is mapped into the reference coordinates of the FFD (s, t, p) unity cube. Consequently, the domain D is in the unity cube reference coordinates, $\Psi : (D) \rightarrow (0,1) \times (0,1) \times (0,1)$. Therefore, selecting unpertubed control points $\mathbf{P}^0_{l,m,n}$, where $l = 0, ..., L, m = 0, ..., M$ and $n = 0, ..., N$, it can be written that:

$$\mathbf{P}^0_{l,m,n} = \begin{bmatrix} l/L \\ m/M \\ n/N \end{bmatrix} . \tag{6}$$

Each control point can potentially move in three distinct directions, s, t and p. A parameter vector $\boldsymbol{\mu}_{l,m,n}$ is introduced to account for this consideration and it is visually depicted in Fig. 2

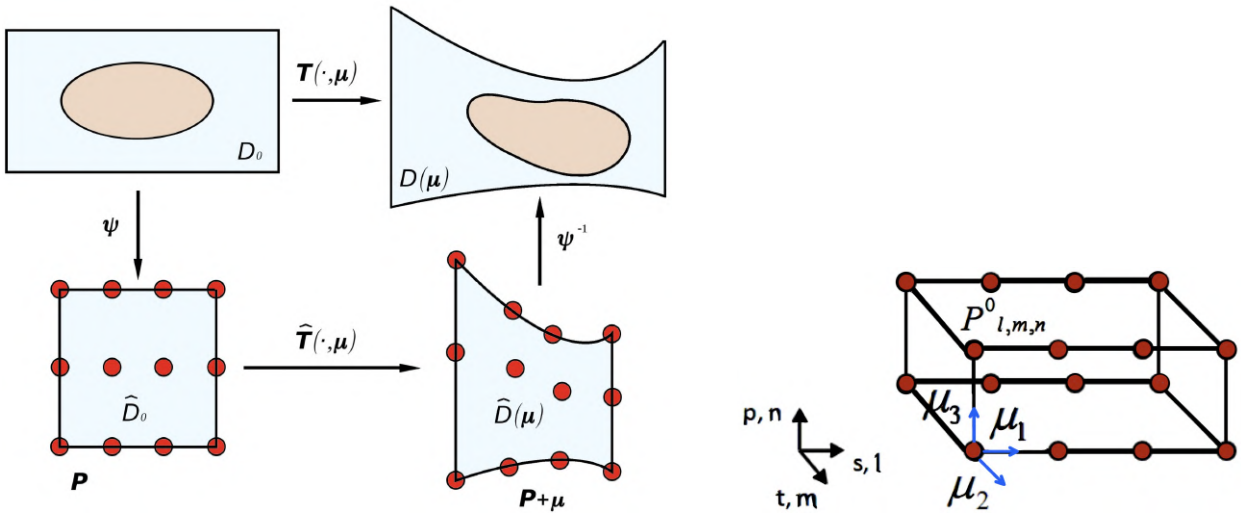

(a) Sketch of the 2-D FFD map construction.

(b) Unperturbed control points and parameters vector for 3-D case.

Figure 2. FFD map representation.

The corresponding value of the parameters vector pertubs each control point as follows:

$$\mathbf{P}_{l,m,n}\left(\boldsymbol{\mu}_{l,m,n}\right) = \mathbf{P}^0_{l,m,n} + \boldsymbol{\mu}_{l,m,n} . \tag{7}$$

Therefore, the parametric domain map, $\mathbf{T} : D_0 \rightarrow D(\boldsymbol{\mu})$, can be constructed as

$$\mathbf{T}\left(\Psi(x); \boldsymbol{\mu}\right) = \Psi^{-1}\left(\sum_{l=0}^{L}\sum_{m=0}^{M}\sum_{n=0}^{N} b^{L,M,N}_{l,m,n}(s,t,p)\mathbf{P}_{l,m,n}(\boldsymbol{\mu}_{l,m,n})\right) \tag{8}$$

where $b^{L,M,N}_{l,m,n}(s,t,p)$ are tensor products of the 1-d Berstein polynomials defined with local variables on the unit square as previously mentioned $(s,t,p) \in [0,1] \times [0,1] \times [0,1]$, written as

$$b^{L,M,N}_{l,m,n}(s,t,p) = b^L_l(s) b^M_m(t) b^N_n(p) , \tag{9}$$

$$b_l^L(s)b_m^M(t)b_n^N(p) = \begin{pmatrix} L \\ l \end{pmatrix} \begin{pmatrix} M \\ m \end{pmatrix} \begin{pmatrix} N \\ n \end{pmatrix} (1-s)^{(L-l)} s^l (1-t)^{(M-m)} t^m (1-p)^{(N-n)} p^n \,, \tag{10}$$

where each tensor product can be written as:

$$b_l^L(s) = \begin{pmatrix} L \\ l \end{pmatrix} (1-s)^{L-l} s^l \,,$$

$$b_m^M(t) = \begin{pmatrix} M \\ m \end{pmatrix} (1-t)^{M-m} t^m \,, \tag{11}$$

$$b_n^N(p) = \begin{pmatrix} N \\ n \end{pmatrix} (1-p)^{N-n} p^n \,.$$

In order to effectively compute the global map $\mathbf{T}$, it involves two main components, namely the offline phase and the online phase. The offline phase entails precomputing the transformation through the utilization of a symbolic expression. Conversely, the online phase involves evaluating the function for the system's parameters and coordinates. Remarkably, the latter part is relatively inexpensive, even in scenarios involving three-dimensional data. Consequently, once the offline phase, which incurs the majority of the computational cost, is completed, the map $\mathbf{T}$ can be readily calculated by simply evaluating it (Koshakji *et al.*, 2013). This characteristic renders it a valuable tool for optimization problems that require repeated computations.

2.4 Scipy Minimization

The sequential least-squares quadratic programming (SLSQP) method, originally formulated by Kraft (1994), offers an iterative approach to solving nonlinear optimal control problems with a set of constraints. This method is applicable when both the objective and constraint functions possess second-order continuous differentiability. Notably, the SLSQP method addresses large-scale optimization problems by solving a sequence of optimization sub-problems at each time step, as expounded upon by Nocedal and Wright (2006).

In the current study, the SLSQP minimization algorithm is adopted from the Scipy (Scientific Computing in Python) Python library (Virtanen *et al.*, 2020). The selection of the Scipy Python library is primarily driven by its robustness and its capability in handling constrained functions. Furthermore, it is imperative to underscore that the implementation of this library mandates the existence of design variables constrained within specified bounds, thereby ensuring the accurate computation of the merit function minimization. This characteristic is intricately aligned with the overarching objectives of the ongoing investigation.

3. RESULTS

3.1 FFD Verification

The verification process of the free form deformation code focuses on the parameterization of the NASA Common Research Model, CRM. The FFD lattice encompasses control volumes that correspond to the coordinates of each grid point within the generated CRM mesh Fig. 3a. Notably, when the control points, highlighted in red in Fig. 3b, experience a specified displacement, the grid undergoes deformation within a three-dimensional trivariate Bezier volumes.

3.2 UVLM Validation

The validation of the unsteady vortex lattice method relies on the examination of the high-lift propeller, HLP, utilized in the NASA X-57 Maxwell aircraft (Borer *et al.*, 2016). The HLP has a radius denoted as $R = 0.2880$ m, and consists of five blades featuring a uniform MH-114 airfoil configuration throughout the radial span. The validation process is carried out under the HLP's design condition characterized by an operational speed of 4550 rpm, an incoming flow velocity denoted as $V_\infty = 29.8$ m/s, and a standard atmospheric density represented as $\rho_\infty = 1.225$ kg/m^3. A comparison is made between the observed wake topology and the outcomes obtained by Fei *et al.* (2022) utilizing the $RoBIN$ code. The current unsteady wake outcomes were acquired by conducting two complete rotor revolutions, each consisting of 72 azimuths. Each blade mesh encompasses 9 chordwise and 13 spanwise vortex ring elements. The RoBIN outcomes (Fei *et al.*, 2022) employed a mesh with 20 by 20 vortex ring elements, covering 8 complete revolutions with 72 azimuths each. Despite employing fewer rotor revolutions and a coarse mesh to reduce computational cost, the obtained wake structure, Fig. 4a demonstrates a satisfactory agreement with the reference, Fig. 4b, across all angles of attack, even in the most challenging case of 60 degrees.

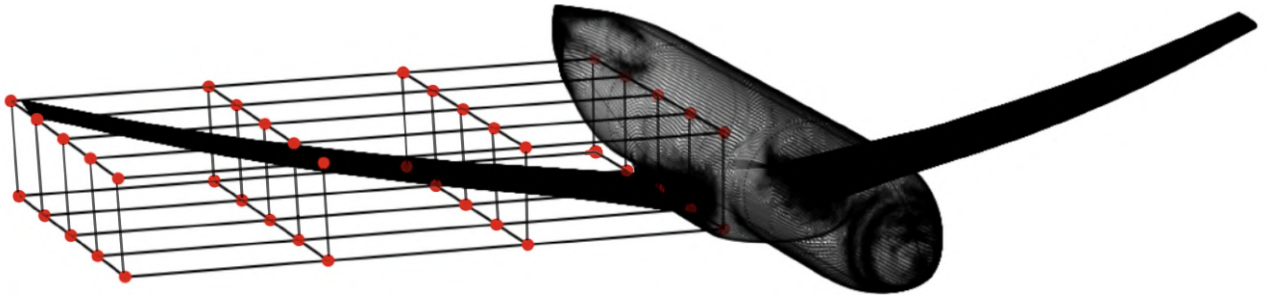

(a) Unperturbed FFD control points.

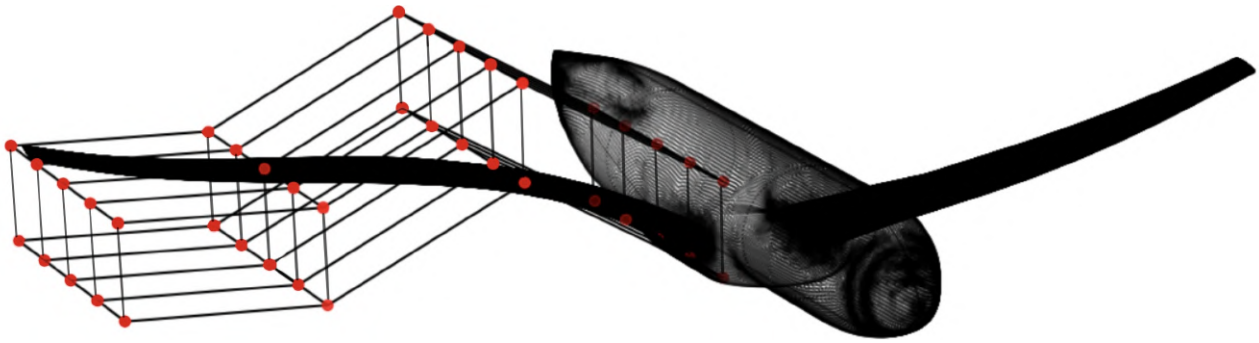

(b) Perturbed FFD control points section.

Figure 3. CRM FFD parametrization.

Figure 5 illustrates a comparative analysis between the current code and the RoBIN and Overflow isolated propeller results, obtained by Fei *et al.* (2022), across a range of α_p values. While the integration of viscous corrections exhibited strong concordance with Overflow results at low angles of attack, an absence of stall capture indicates the need for a reevaluation of the decambering method implementation for more aggressive angles of attack . Nevertheless, generally favorable agreement was observed between the current code and both reference codes, particularly in terms of forces and moments at low angles of attack

3.3 Optimization

In the context of electric vertical take-off and landing (eVTOL) aircraft, it is of utmost importance for the designers not only to strive for enhanced rotor performance but also to mitigate the adverse effects of rotor wake on the airframe, particularly on the wing. The present study explores into the examination of optimization parameters that can potentially contribute to the reduction of the induced angle of attack experienced by the wing. By minimizing the induced angle of attack, each wing section can be shielded from early stall conditions. This research specifically investigates the independent variations of pitch angle and chord length for each UVLM rotor panel, aiming to discern the impact of rotor wake changes and determine the most influential parameter for achieving a significant reduction in the induced angle of attack on the wing. The validity of the study is ascertained through an examination of the variation in wake topology, with the same mesh size and time step discretization as used in Subsection 3.2

Both pitch angle and chord length of each rotor section were reduced by approximately 50%, and the resulting wake patterns, for a rotor angle of attack of 60°, for each case are illustrated in Fig. 5. Upon observation, it is evident that the variation in chord length has a significant influence on the changes in wake topology compared to the modifications in pitch angle. Conversely, the optimization sensitivities mainly revolve around managing the chord length to ensure minimal impact on rotor performance while at the same time minimal interference with the vehicle's wing. In this way, it is necessary to make a deeper trade-off considering more design variables.

4. CONCLUDING REMARKS

The results presented in this work addressed a 3-D parameterization and unsteady simulation performed using the Free-Form-Deformation methodology and the unsteady vortex lattice method, respectively. Moreover, tackled the verification of the sensitivity of some geometric parameters in the optimization process using the implemented parameterization and simulation tools. The calculations have used a Fortran code for the description of the aerodynamics, and the parameterization module and optimization itself have been treated with a Python script. The results obtained so far seem to be in line with what one should expected for the physics of the problem and the aerodynamic description of the problem that has been used. These results also show that there is an opportunity for implementing the aerodynamic shape optimization framework for more complex rotor-wing interaction problems.

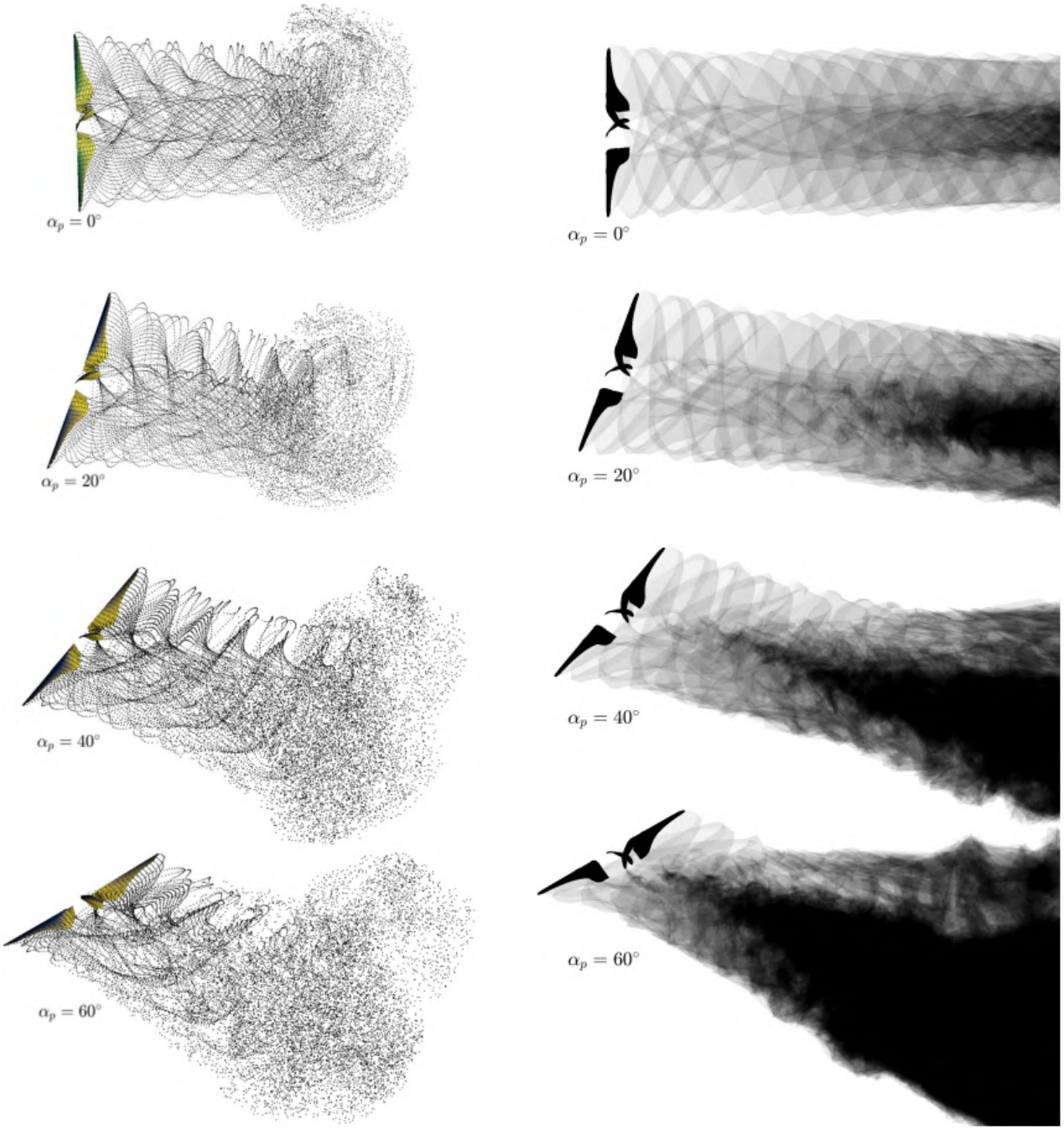

(a) Present work with 2 complete revolutions. (b) RoBIN code with 8 complete revolutions.

Figure 4. Wake distortion with propeller angle of attack, α_p.

In the subsequent research endeavors, a more comprehensive optimization study incorporating a broader range of design parameters should be carried out. Furthermore, the ultimate objective entails extending the analysis to a more challenging configuration, involving a wing-mounted multiple rotor coupling, where the primary focus of this investigation should pertains to the analysis of the wing's transition operation from hover to cruise mode.

5. ACKNOWLEDGEMENTS

The authors gratefully acknowledge the support for the present research provided by Conselho Nacional de Desenvolvimento Científico e Tecnológico, CNPq, under the Research Grant No. 309985/2013-7. The work is further supported by Fundação de Amparo à Pesquisa do Estado de São Paulo, FAPESP, under the Research Grant No. 2013/07375-0.

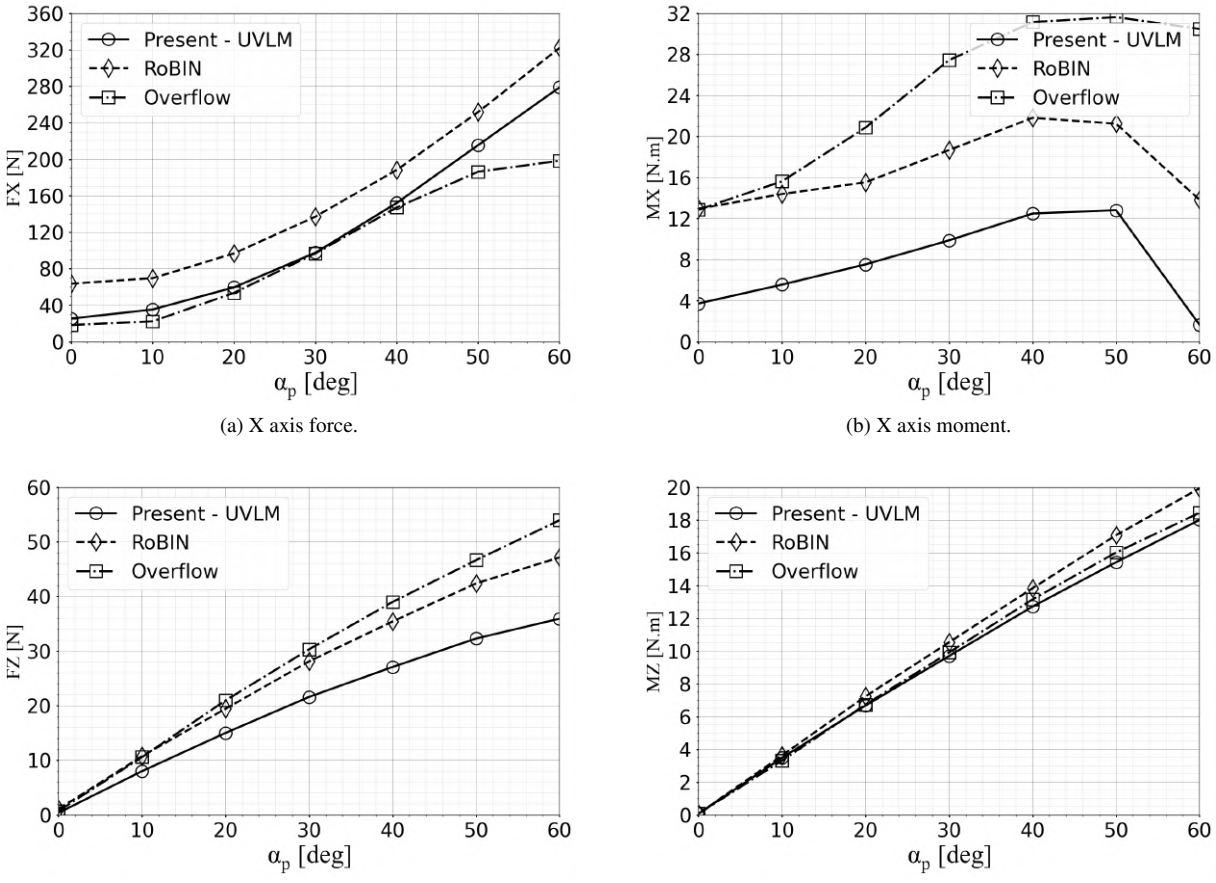

(a) X axis force.

(b) X axis moment.

(c) Z axis force.

(d) Z axis moment.

Figure 5. Comparison of present work with RoBIN and OVERFLOW code results for the isolated HLP over a sweep of α_p.

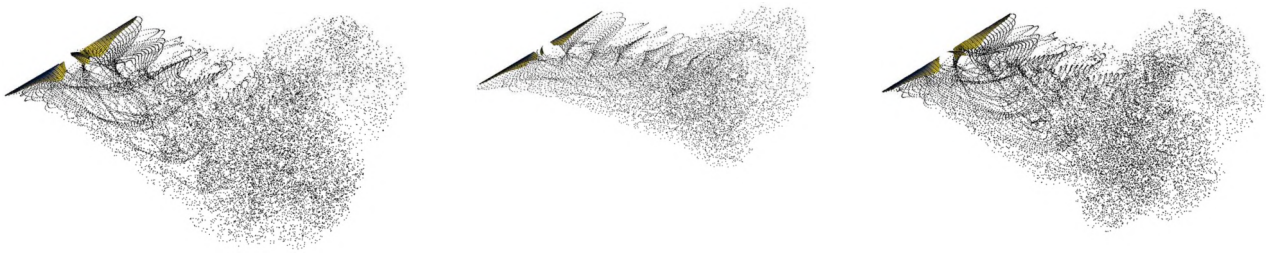

(a) Original geometry.

(b) 50% chord length reduction.

(c) 50% pitch angle reduction.

Figure 6. Wake topology effect due to pitch angle and chord length variation of each rotor section for $\alpha_p = 60°$.

6. REFERENCES

Bhagwat, M. and Leishman, J.G., 2000. "Time-Accurate Modeling of Rotor Wakes Using a Free-Vortex Wake Method". In *in Proceedings of the Specialist Meeting of the American Helicopter Society*. Virginia Beach, Va, USA.

Borer, N., Patterson, M., Viken, J., Moore, M., Bevirt, J., Stoll, A. and Gibson, A., 2016. "Design and Performance of the NASA SCEPTOR Distributed Electric Propulsion Flight Demonstrator".

Cohen, E., Riesenfeld, R.F. and Gershon, E., 2002. *Geometric Modeling with Splines: An Introduction*. AK Peters Natick, Massachusetts, USA.

Drela, M., 1989. "XFOIL: An Analysis and Design System for Low Reynolds Number Airfoils". In T.J. Mueller, ed., *Low Reynolds Number Aerodynamics*. Springer-Verlag, New York, USA, Vol. 54 of *Lecture Notes in Engineering*, pp. 1–12.

Erhard, R.M. and Alonso, J.J., 2022. "A comparison of Propeller Wake Models for Distributed Electric Propulsion and eVTOL Aircraft in Complex Flow Conditions". In *AIAA SCITECH 2022 Forum*. p. 1676.

Fei, X., Litherland, B.L. and German, B.J., 2022. "Development of an Unsteady Vortex Lattice Method to Model Propellers at Incidence". *AIAA Journal*, Vol. 60, No. 1, pp. 176–188. doi:10.2514/1.J060133.

Hess, J. and Smith., A., 1967. "Calculation of Potential Flow About Arbitrary Bodies". *Progress in Aerospace Sciences*, Vol. 8, pp. 1–138. doi:10.1016/0376-0421(67)90003-6.

Katz, J. and Plotkin, A., 2004. *Low-Speed Aerodynamics, Second Edition*. Cambridge University Press, Massachusetts, USA.

Konstadinopoulos, P., Thrasher, D.F., Mook, D.T., Nayfeh, A.H. and Watson, L., 1985. "A Vortex-Lattice Method for General, Unsteady Aerodynamics". *Journal of Aircraft*, Vol. 22, No. 12, pp. 43–49.

Koshakji, A., Quarteroni, A. and Rozza, G., 2013. "Free Form Deformation Techniques Applied to 3D Shape Optimization Problems". *Communications in Applied and Industrial Mathematics*, Vol. 4.

Kraft, D., 1994. "Algorithm 733: TOMP–Fortran Modules for Optimal Control Calculations". *ACM Transactions on Mathematical Software*, Vol. 20, No. 3, pp. 262–281.

Mukherjee, R. and Gopalarathnam, A., 2006. "Post-Stall Prediction of Multiple-Lifting-Surface Configurations Using a Decambering Approach". *Journal of Aircraft*, Vol. 43, No. 3, pp. 660–668. doi:10.2514/1.15149.

Nocedal, J. and Wright, S., 2006. *Numerical Optimization*. Springer, New York.

Perry, E.W. and Balling, R., 1998. "A New Morphing Method for Shape Optimization". In *7th AIAA/USAF/NASA/ISSMO Symposium on Multidisciplinary Analysis and Optimization*. doi:10.2514/6.1998-4907.

Samareh, J.A., 2000. "Multidisciplinary Aerodynamic-Structural Shape Optimization Using Deformation (MASSOUD)". In *8th Symposium on Multidisciplinary Analysis and Optimization*. Long Beach, CA, USA. doi:10.2514/6.2000-4911.

Sedeberg, T.W. and Parry, S.R., 1986. "Free-Form Deformation of Solid Geometric Models". *ACM Siggraph Computer Graphics*, Vol. 20, pp. 151–160.

Virtanen, P., Gommers, R., Oliphant, T.E., Haberland, M., Reddy, T., Cournapeau, D., Burovski, E., Peterson, P., Weckesser, W., Bright, J., van der Walt, S.J., Brett, M., Wilson, J., Jarrod Millman, K., Mayorov, N., Nelson, A.R.J., Jones, E., Kern, R., Larson, E., Carey, C., Polat, İ., Feng, Y., Moore, E.W., van der Plas, J., Laxalde, D., Perktold, J., Cimrman, R., Henriksen, I., Quintero, E.A., Harris, C.R., Archibald, A.M., Ribeiro, A.H., Pedregosa, F. and van Mulbregt, P., 2020. "SciPy 1.0: Fundamental Algorithms for Scientific Computing in Python". *Nature Methods*, Vol. 17, No. 3.

Weissinger, J., 1947. "The Lift Distribution of Swept-Back Wings". *National Advisory Committee for Aeronautics. Langley Aeronautical Lab. Langley Field*.

Wie, S.Y., Lee, S. and Lee, D., 2009. "Potential Panel and Time-Marching Free-Wake Coupling Analysis for Helicopter Rotor". *Journal of Aircraft*, Vol. 46, No. 3, pp. 1030–1041.

7. RESPONSIBILITY NOTICE

The authors are solely responsible for the printed material included in this paper.